



A microscopic view of particle bombardment of organic films

Ramona S. Taylor, Barbara J. Garrison*

Department of Chemistry, 152 Davey Laboratory, The Pennsylvania State University, University Park, PA 16802, USA

Received 12 August 1994; accepted 27 October 1994

Abstract

The high energy particle bombardment of molecular films adsorbed upon a metal substrate has been investigated via molecular dynamics computer simulations with an empirical many-body potential function constructed for studying reactive dynamics. These calculations identify lateral motion of fragments in the overlayer as giving rise to fragmentation and direct abstraction type reactions. In addition, the importance of substrate mass for particle ejection is identified. These concepts are discussed in detail and experiments are proposed to test these ideas.

Keywords: Molecular dynamics; Organic overlayers; Particle bombardment; Sputtering

1. Introduction

The technical developments and applications of kiloelectronvolt particle bombardment techniques such as secondary ion mass spectrometry and fast atom bombardment mass spectrometry, perhaps in conjunction with laser post-ionization, are booming as evidenced by the articles in this tissue. Concomitant with experimental developments has been a surge in the use of molecular dynamics (MD) simulations to model experimental events [1–18]. MD simulations provide valuable information about the mechanisms and pathways of atomic motions by which reactions can occur. The strength of the MD approach is that it allows one to view the atomic motions and also calculate quantities that can be

directly compared to experimental results. An added feature of MD simulations is the capability to alter characteristics of the system that cannot be easily varied experimentally in order to gain mechanistic insight into fundamental events.

MD simulations have long been used to model the early stages, i.e. the first 0.5–1 ps, of the high energy bombardment process. Early investigations using simple pairwise additive potentials surprisingly were able to reproduce many of the experimental observations thought to be important to the high energy bombardment process of single-crystal metal and semiconductor surfaces [2]. Even the simulations of organic films such as benzene, pyridine and coronene adsorbed on Ni identified important mechanistic variables leading to the ejection of the cationized and intact adsorbates [17]. These simulations show that

* Corresponding author.

the molecular species is often ejected intact because a moving Ni atom can simultaneously contact two or more C atoms and concertedly push them in one direction rather than automatically severing a bond. In addition, the large number of internal degrees of freedom possessed by an organic molecule allow it to absorb energy from the impact and consequently not fragment. Simulations of pyridine adsorbed on an Ni surface showed that as the pyridine molecule desorbs it is often channeled in an upward direction by the neighboring pyridine adsorbates [14]. These calculations were limited at the time by the availability of interaction potentials to describe the events of interest. In particular, it was impossible to address the question of reasonable fragmentation channels and reactions between adsorbate molecules [19]. Recently a many-body potential has been developed to allow for reactions between hydrocarbon species [20,21]. It has been used in conjunction [22] with the embedded atom method (EAM) potential [23–25] for Pt in order to investigate the reactions that occur during particle bombardment of organic overlayers on Pt{111}. The model system studied is ethylidyne, C_2H_3 , adsorbed on Pt{111} which has been investigated experimentally in SIMS [26–28]. In addition, we constructed longer-chain analogs, propylidyne (C_3H_5) and pentylidyne (C_5H_9) in order to examine the effect of having a longer hydrocarbon chain.

These calculations represent a major advance in terms of realistically modeling reactions among the organic molecules. The calculations of 10 years ago did not allow for atoms from one hydrocarbon molecule to combine with atoms from another to form a completely new molecule. These MD calculations [22,26–28] are aimed at providing a microscopic view of the reactions among the neutral species in the first 0.5–1 ps of the collision cascade. In particular we are interested in identifying processes that are common among

all the stimulations and which may have broader applicability across different experimental configurations. One common feature identified is lateral motion of both metal atoms and hydrocarbon fragments in the 1–5 Å region above the metal substrate. This motion is due to the collision cascade and consequently some of the particles have kinetic energies sufficient to fragment other molecules or to induce chemical reactions to form new molecules. Consistent with a collision cascade, the time scale of these reactions is well below a picosecond. To get these reactions to occur, one does not have to assume the high temperature and/or pressure often associated with processes that are proposed to occur in the seldge region [29–32]. We also find that the heavy mass of the substrate (Pt vs. C) plays a role in enhancing ejection. We propose experiments to explore further the consequences of these phenomena.

2. Method

The 500 eV Ar bombardment of $p(2 \times 2)$ films of C_2H_3 , C_3H_5 and C_5H_9 molecules adsorbed on Pt{111} are modeled via molecular dynamics (MD) computer simulations. The classical MD scheme has been described in detail elsewhere [3–5,22]. The forces among the various atoms are calculated using a blend of empirical potential energy functions chosen to model as best as is currently feasible in all the possible reaction channels. The Ar–Pt, Ar–C and Ar–H interactions are described using a purely repulsive Molière pairwise potential energy function [33]. For the remainder of the particles, both the repulsive and attractive interactions among the particles are included. The Pt–Pt interactions are described by an attractive, many-body potential function based upon the embedded atom method (EAM) [23–25]. The EAM Pt potential is chosen as energy and angular

distributions calculated from MD simulations of the high-energy bombardment of other f.c.c. metals using the EAM potentials compare well with the corresponding experimental observations [34,35].

The C–C, C–H and H–H interactions are described with a reactive many-body potential energy function developed by Brenner and co-workers [20,21] which not only describes the energetics of bulk diamond and graphite, but also those of a wide array of small hydrocarbon molecules, such as C_2H_4 , C_2H_6 and C_6H_6 , and radicals, such as CH_3 and C_3H_5 . This potential was originally developed to model the chemical vapor deposition of diamond films but, in fact, has been used in a number of simulations of other hydrocarbon interactions and reactions including the insertion of CH_2 into a surface dimer on the diamond $\{001\}$ (2×1)H surface [36]; fullerene formation from graphite ribbons [37] as well as fullerene cage stability [38]; the pick-up of a molecule from a surface by another gas-phase molecule (an Eley–Rideal reaction sequence) [39]; and friction [40] at diamond surfaces. The Pt–H interactions are described with a Lennard–Jones potential and the Pt–C interactions are described via a potential energy function that consists of a Lennard–Jones pairwise component and a many-body component specifically designed to work in conjunction with Brenner's hydrocarbon potential [22]. Due to this many-body component, adsorbates bind in the site which best preserves the sp^3 coordination of the binding C atom. For all the molecules described here, the most stable site is the three-fold hollow as shown in Fig. 1. The binding energy in the three-fold hollow site to the substrate of both the C_2H_3 and C_3H_5 adsorbate is 7.35 eV which is well within the reported range for C_2H_3 of 6.9–8.5 eV [41,42]. As this energy is relatively large compared to the C–C and C–H bond strengths we chose to decrease the Lennard–Jones well depth of the Pt–C potential such

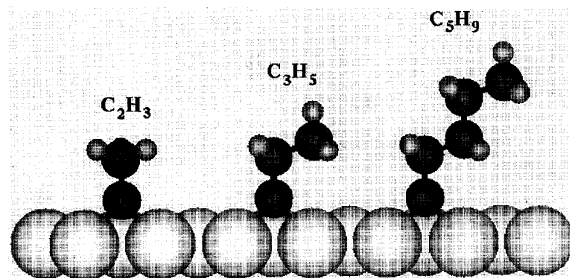


Fig. 1. Geometry of C_2H_3 , C_3H_5 and C_5H_9 on the Pt $\{111\}$ surface. The large light grey spheres represent Pt atoms, the dark grey spheres represent C atoms, and the small medium grey spheres represent H atoms. This color scheme is used throughout this paper.

that the binding energy of each C_5H_9 adsorbate is only 2.70 eV. Due to the short-ranged nature of the Pt–C potential, the binding energies of hydrocarbon films adsorbed in both the h.c.p. and the f.c.c. three-fold sites are equivalent.

The crystal sizes are chosen to be large enough such that the main dynamical effects of the collisional impact are retained for normally incident Ar bombardment at the experimental energy of 500 eV [28]. The Pt– C_2H_3 system is modeled by a microcrystallite containing 1512 Pt atoms uniformly arranged in seven layers and three different C_2H_3 films representing quarter monolayer coverages in f.c.c. and h.c.p. sites and a half monolayer coverage in a honeycomb arrangement [22]. A total of 1390 Ar impacts was calculated. In each case the Ar impacted a pristine sample — the ultimate in static mode. The Pt– C_3H_5 and Pt– C_5H_9 systems are both modeled with a crystallite containing 1998 Pt atoms arranged in six layers and a film consisting of 77 adsorbates. For the C_3H_5 system a total of 500 Ar impacts was calculated. For C_5H_9 , each trajectory requires between 8 and 12 h of CPU time on one node of an IBM SP1 computer and thus only 50 trajectories were calculated. Finally we performed simulations on a clean Pt $\{111\}$ crystal and a clean diamond C $\{111\}$ surface. Each trajectory is terminated when the total energy of any atom remaining in the solid falls below the level where any further ejection

can take place. In all simulations, open boundary conditions are used [3–5].

3. Results and discussion

The focus of the discussion revolves around the lateral motion in the 1–5 Å region above the metal substrate in the cascade and how this motion affects the fragmentation process and reactions. In addition, the role of substrate mass is examined. From these observations in the calculations come natural suggestions of possible experiments. As a reminder to the reader, the discussion below relates to the first picosecond of the collision cascade.

3.1. Lateral motion induced fragmentation

In the MD simulations of the 500 eV Ar bombardment of C₂H₃, C₃H₅ and C₅H₉ adsorbed on Pt{111}, the lateral motion of the ejecting particles is a major dynamical factor in the fragmentation of the existing adsorbates. As ejecting particles, either Pt or CH_x species, desorb from the surface, they collide with and cause the fragmentation of other adsorbates [43]. The collisions between the ejecting species and the as of yet undisturbed adsorbate molecules often result in the cleavage of the adsorbate. Given in Table 1 are the origins of the more common C_xH_y species observed in the simulations. The larger species (relative to the original adsorbate molecule) tend to be the top portion of the adsorbates. For example, 93% of the C₃H₇ species observed in the C₅H₉ simulations originate from the three carbon atoms farthest from the Pt surface. More than 75% of the CH₃ species in all the simulations come from the top carbon. As the species becomes smaller, e.g. CH₂, it becomes much more difficult to relate them back to one portion of the original adsorbate.

3.2. Lateral motion induced reactions

The lateral motion of the ejecting particles also plays a role in determining the nature of the ejected particles. As the ejecting particles move across the surface, instead of the collision induced fragmentation there can be a combinative reaction between the colliding particle and the adsorbate. In the example shown in Fig. 2 from the bombardment of the C₂H₃ overlayer, an ejecting CH₃ species is created by the collision of the incoming Ar beam with a C₂H₃ adsorbate. This CH₃ species is subsequently propelled laterally across the surface until it finally collides and subsequently reacts with another as of yet undisturbed C₂H₃ adsorbate. The CH₃ species abstracts a hydrogen atom from this second C₂H₃ adsorbate to form CH₄. If the initial CH₃ species had been ejected vertically from the surface, the formation of a species such as CH₄ would likely not have occurred. All of the CH₄ detected in the bombardment of C₂H₃ and C₃H₅ films originates from the addition of a single H atom to the top CH₃ species. This reaction only requires the collision of two species, whereas the formation of CH₄ from perhaps the addition of two H atoms to a CH₂ species would require two collisions. Multiple collisions with the right characteristics to lead to reaction have a much lower probability for occurrence. A similar H abstraction process has been discussed earlier for the formation of H₂ [44]. Reactions of this type are responsible for the formation of some fraction of the following species in the C₂H₃ study — H₂, CH₄, HCCH₂, H₂CCH₂ and HCCH₃. As reported in an earlier work the simulations predict that some of the first three species will be stable and that the latter three species will fragment or rearrange before they can be detected [22].

It should be possible to test some of the proposed mechanisms associated with lateral motion. For example, if the top C of the chains

Table 1
Percentage of ejected species originating from one adsorbate

Detected species	Origin	% of total formed		
		C ₂ H ₃	C ₃ H ₅	C ₅ H ₉
CH ₂	C ^{N-3} H ₂	—	—	16
CH ₂	C ^{N-2} H ₂	—	—	16
CH ₂	C ^{N-1} H ₂	—	38	32
CH ₃	C ^N H ₃	99	95	78
CH ₄	C ^N H ₃ + H	100	100	—
C ₂ H ₂	C ⁰ C ⁰⁺¹ H ₂	—	20	70
C ₂ H ₄	C ^{N-1} H ₂ C ^N H ₃ - H	—	88	40
C ₂ H ₄	C ^{N-2} H ₂ C ^{N-1} H ₂	—	—	53
C ₂ H ₅	C ^{N-1} H ₂ C ^N H ₃	—	96	100
C ₃ H ₇	C ^{N-2} H ₂ C ^{N-1} H ₂ C ^N H ₃	—	—	93

C^N signifies topmost carbon atom in linear chain, i.e. C^N in the C₅H₉ molecule would be the C⁵ carbon atom while C^N in the C₃H₅ adsorbate would be the C³ carbon atom. Similarly, C⁰ signifies the binding C atom.

shown in Fig. 1 were deuterated then the ratio of CD₃ vs. CD₂H, CDH₂ and CH₃ measured would indicate the amount of shearing off of the top methyl group vs. formation from other pathways. One could also look for CD₄ or CD₃H as indicators of reactions between adsorbate molecules. The above experiments are proposed assuming the experimentalists can make and detect any molecule, neutral or ionic. In fact making pure C₂D₃ on a Pt surface might be very challenging as considerable H atom exchange occurs with bulk hydrogen. The synthesis of CH₂=CH-CD₃ or CH₂=CH-CH₂-CH₂-CD₃, the known precursor of propylidyne and a proposed precursor of pentylidyne, might be more tractable. Moreover, self-assembled monolayers of alkane thiols [45] provide a wealth of possibilities of various chain lengths and end groups for testing of the ideas presented here. Of note is that the deuteration (or perhaps fluorination) scheme suggested here is different to those that have been performed [46,47]. Specifically we are suggesting that one C along the chain be deuterated rather than the whole chain. In this way the position of the fragments can be determined.

3.3. Substrate mass effect

The nature of the substrate also affects the desorption process. Calculations with C₅H₉ adsorbed on both Pt{111} and diamond (C{111}) substrates show the total yield of ejected particles is much lower for the diamond substrate than for platinum [48]. For instance, the yield of ejected H atoms falls from 23 H atoms per incident Ar particle with a Pt substrate to 2 H atoms per incident Ar particle with a diamond substrate. The difference in yields for the Pt (195 u) and C (12 u) substrates is due to the inability of the diamond substrate to redirect the momentum of the incoming Ar (40 u) atom upward. As a computational test of this idea, we performed calculations for the clean Pt and diamond systems in which we artificially exchange the masses, i.e. we created the rare ¹⁹⁵C and ¹²Pt isotopes, while not altering the respective crystal structures or interaction potentials. Fig. 3 shows the same trajectory (i.e. same initial impact point of the Ar atoms) for both the

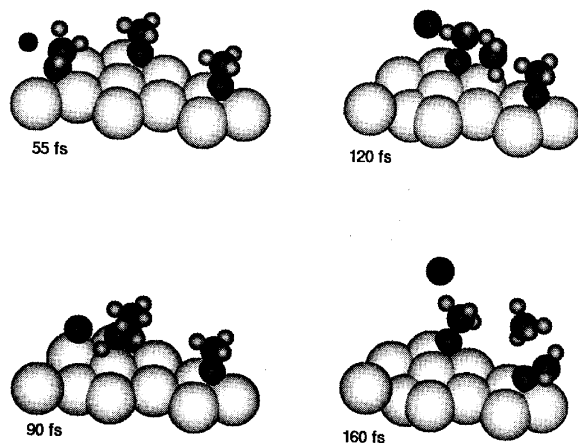


Fig. 2. Hydrogen abstraction reaction by a free CH₃ radical which leads to the formation of CH₄. The CH₃ radical results from the collision of the incoming Ar atom with the C₂H₃ adsorbate on the left. An H atom is abstracted from the C₂H₃ adsorbate on the right. The middle C₂H₃ adsorbate is out of the plane of the two reacting C₂H₃ molecules and does not enter into the reaction. See text for a description of the collision events.

$^{12}\text{C}\{111\}$ and $^{195}\text{C}\{111\}$ crystal. The interactions between the Ar beam and the crystals are identical, but less than 80 fs into the trajectory the crystals are behaving quite differently. While the ^{12}C crystal shows only slight perturbation of the top layer C atoms, the ^{195}C crystal shows ejection of C atoms. At 320 fs, the ^{195}C crystal continues to lose C atoms, while the ^{12}C crystal actually shows an annealing of the damaged top layers. The Ar atom passes through the ^{12}C crystal but is reflected back out of the ^{195}C crystal. Similar calculations for the clean ^{12}Pt crystal again show that as the mass of the Pt atoms is lowered from 195

to 12 u, the yield of ejected particles decreases. The main point of Fig. 3(a) is that for the $^{12}\text{C}\{111\}$ system there is no removal of material and the sample near the surface has almost returned to its crystalline state in a very short time. For $^{195}\text{C}\{111\}$ as shown in Fig. 3(b), there is removal of material from the system. The light mass of ^{12}C is ineffectual at redirecting the momentum of the heavier ^{40}Ar . As an aside, these simulations on mass effect point out one utility of computer simulations. We are able to change only the mass of the substrate while keeping all other conditions such as interaction potential and crystal

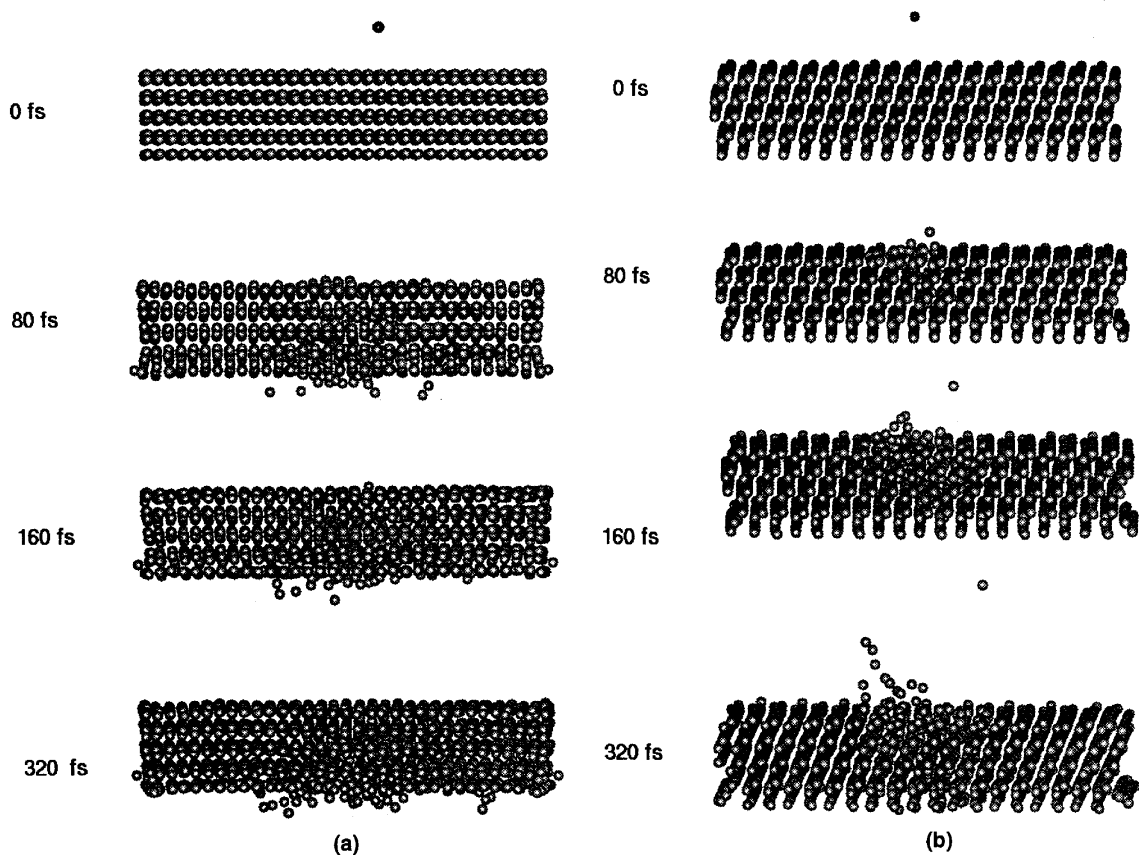


Fig. 3. (a) Clean $^{12}\text{C}\{111\}$ crystal. The Ar atom (small black sphere) penetrates the diamond lattice (grey spheres) and causes no ejection of the substrate. (b) Clean $^{195}\text{C}\{111\}$ crystal. Except for the mass of the individual C atoms, this trajectory is identical to that in (a). Here, ejection of the substrate does occur. See text for explanation of the collisional events. The particles that appear to come out of the bottom of the crystal would actually disrupt deeper levels of the solid. We test the number of atoms that are used in the simulation in order to make sure this motion does not affect the ejection process.

structure constant. Unfortunately this is almost impossible to do experimentally.

There are numerous SIMS experiments of molecular species in which a metal substrate is used. The main utility though has been thought to be as a means of cationizing the parent molecule for easy detection. These MD simulations suggest that a substrate which is heavier than the incident particle is more effective at redirecting the downward momentum of the incident particle than a lightweight substrate. It might, in fact, be advantageous to intentionally insert a metal layer to enhance the total yield of particles that are ejected.

4. Conclusion

The results presented here are from massive molecular dynamics calculations aimed at describing unknown *reactive* dynamics among a multitude of atoms in a complex environment. In particular, we have modeled the 500 eV Ar bombardment of C_2H_3 , C_3H_5 , and C_5H_9 adsorbed on a Pt{111} surface and monitored the reactions induced by the collision cascade. The calculations predict the presence of lateral motion of substrate atoms and fragments of the overlayer which can both cause further fragmentation of the molecules and also induce reactions. We observe a preferential cleavage and subsequent ejection of the top portion of the chains. We also observe abstraction reactions where a species such as H or CH_3 which has been knocked off from one molecule moves laterally across the surface and abstracts a portion of a stationary molecule to form gaseous species such as H_2 or CH_4 . These reactions occur during the collision cascade without invoking the high pressure and/or temperature conditions associated with the selvedge region [29–32].

The strength of the MD approach for examining the particle bombardment process

is the microscopic detail that comes from the atomic positions as a function of time. The assumptions are that the interaction potential is valid and that classical mechanics is valid. All subsequent atomic motions including reactions result without any human intervention about assumed mechanisms. It is these concepts from these simulations that hopefully will aid in the interpretation of experimental results and perhaps inspire new experiments. Experiments to test some concepts here are being planned at both Penn State and UMIST.

The limitations of the method with respect to modeling of particle bombardment include the inability to describe long (i.e. longer than nanosecond) time scales and the lack of electronic effects. The first limitation has ramifications in both predicting the decay process during the flight of any species toward the detector and with modeling directly any long term thermal spike or selvedge region. The decay process especially for the experimental techniques that measure the neutral species can be reasonably estimated given that the MD approach yields the internal energies [22] and it is relatively straightforward to determine with molecules will decompose. The importance of modeling long term processes such as thermal spikes ultimately depends on how many of the observable quantities can be explained by a collision cascade alone.

Incorporation of electronic effects is a challenge. It is our belief that semi-empirical electronic structure techniques such as MNDO [49] are sufficiently good and computationally efficient for small portions of the collision cascade to be modeled by calculating the energies and forces during the MD trajectory [50]. In this vein, the MD simulations presented here provide suggestions for calculations. For example, one could examine the fragmentation and reaction channels of an adsorbate molecule due to collisions with laterally moving species. It is even practical to include charged

species and other elements in the calculations. These issues will certainly be a part of future modeling efforts.

Acknowledgments

The financial support of the National Science Foundation and the IBM Selected University Research program is gratefully acknowledged. The Pennsylvania State University supplied a generous grant of computer time for these calculations. We thank Nicholas Winograd, John C. Vickerman, Josef Michl, Chris L. Brummel, David E. Sanders and Donald W. Brenner for insightful discussions.

References

- [1] P. Sigmund (Ed.), *Fundamental Processes in Sputtering of Atoms and Molecules (SPUT92)*, Symposium on the Occasion of the 250th Anniversary of the Royal Danish Academy of Sciences and Letters, Copenhagen, 30 August–4 September 1992.
- [2] N. Winograd and B.J. Garrison, in A.W. Czanderna and D.M. Hercules (Eds.), *Ion Spectroscopies for Surface Analysis*, Plenum, New York, 1991, p. 45.
- [3] D.E. Harrison, Jr., *CRC Crit. Rev. Solid State Mater. Sci.*, 14 (1988) 51.
- [4] B.J. Garrison, *Chem. Soc. Rev.*, 21 (1992) 155.
- [5] B.J. Garrison, N. Winograd and D.E. Harrison, Jr., *J. Chem. Phys.*, 69 (1978) 1440.
- [6] L.L. Lauderback, M.L. Ang and H.C. Murray, *J. Chem. Phys.*, 93 (1990) 6041.
- [7] K.E. Foley, N. Winograd, B.J. Garrison and D.E. Harrison, Jr., *J. Chem. Phys.*, 80 (1984) 5254.
- [8] D.W. Brenner and B.J. Garrison, *Phys. Rev. B*, 34 (1986) 5782.
- [9] W. Husinsky, G. Nicolussi and G. Betz, *Nucl. Instrum. Methods Phys. Res. B*, 92 (1993) 323.
- [10] P. Wurz, W. Husinsky and G. Betz, *Appl. Phys. A*, 52 (1991) 213.
- [11] H.M. Urbassek, *Nucl. Instrum. Methods Phys. Res. B*, 18 (1987) 587.
- [12] A. Wucher and B.J. Garrison, *Surf. Sci.*, 260 (1992) 257.
- [13] R. Smith, D.E. Harrison, Jr., and B.J. Garrison, *Phys. Rev. B*, 40 (1989) 93.
- [14] D.W. Moon, N. Winograd and B.J. Garrison, *Chem. Phys. Lett.*, 114 (1985) 237.
- [15] R.A. Stansfield, K. Broomfield and D.C. Clary, *Phys. Rev. B*, 39 (1989) 7680.
- [16] M.H. Shapiro and T.A. Tombrello, *Nucl. Instrum. Methods Phys. Res. B*, 90 (1994) 473.
- [17] B.J. Garrison, *J. Am. Chem. Soc.*, 102 (1980) 6553; 104 (1982) 6211; *Int. J. Mass Spectrom. Ion Phys.*, 53 (1983) 243.
- [18] R.P. Webb and D.E. Harrison, Jr., *Phys. Rev. Lett.*, 50 (1983) 1478.
- [19] The potentials of a decade ago did allow for bonds to break so it was possible to discern if a molecule was hit sufficiently hard for fragmentation but it was not possible for bonds to form between atoms that were not originally bonded together.
- [20] D.W. Brenner, *Phys. Rev. B*, 42 (1990) 9458.
- [21] D.W. Brenner, J.A. Harrison, C.T. White and R.J. Colton, *Thin Solid Films*, 206 (1991) 220.
- [22] R.S. Taylor and B.J. Garrison, *Langmuir*, submitted for publication.
R.S. Taylor, Ph.D. Thesis, Pennsylvania State University, 1994.
- [23] S.M. Foiles, M.I. Baskes and M.S. Daw, *Phys. Rev. B*, 33 (1986) 7983.
- [24] M.S. Daw and M.I. Baskes, *Phys. Rev. B*, 29 (1984) 6443.
- [25] M.S. Daw and M.I. Baskes, *Phys. Rev. Lett.*, 50 (1983) 1285.
- [26] J.R. Creighton and J.M. White, *Surf. Sci.*, 129 (1983) 327.
- [27] K.M. Ogle and J.M. White, *Surf. Sci.*, 165 (1986) 234.
- [28] K.M. Ogle, J.R. Creighton, S.A. Akhter and J.M. White, *Surf. Sci.*, 169 (1986) 246.
- [29] F. Honda, G.M. Lancaster, Y. Fukuda and J.W. Rabalais, *J. Chem. Phys.*, 69 (1978) 4931.
- [30] S.J. Pachuta and R.G. Cooks, *Chem. Rev.*, 87 (1987) 647 and references cited therein.
- [31] H.T. Jonkman, J. Michl, R.N. King and J.D. Andrade, *Anal. Chem.*, 50 (1978) 2078.
- [32] R.J. Day, S.E. Unger and R.G. Cooks, *Anal. Chem.*, 52 (1980) 557A.
- [33] D.J. O'Connor and R.J. Macdonald, *Radiat. Eff.*, 34 (1977) 247.
- [34] B.J. Garrison, N. Winograd, D.M. Deaven, C.T. Reimann, D.Y. Lo, T.A. Tombrello, D.E. Harrison, Jr., and M.H. Shapiro, *Phys. Rev. B*, 37 (1988) 7197.
- [35] A. Wucher and B.J. Garrison, *Surf. Sci.*, 260 (1992) 257.
- [36] B.J. Garrison, E.J. Dawnaski, D. Srivastava and D.W. Brenner, *Science*, 255 (1992) 835.
- [37] D.H. Robertson, D.W. Brenner and C.T. White, *J. Phys. Chem.*, 96 (1992) 6133.
- [38] A. Maiti, C.J. Brabec and J. Bernholc, *Phys. Rev. Lett.*, 70 (1993) 3023.
- [39] E.R. Williams, G.C. Jones, Jr., L. Fang, R.N. Zare, B.J. Garrison and D.W. Brenner, *J. Am. Chem. Soc.*, 114 (1992) 3207.
- [40] (a) J.A. Harrison, C.T. White, R.J. Colton and D.W. Brenner, *Phys. Rev. B*, 46 (1992) 9700.
(b) S.B. Sinnott, R.J. Colton, C.T. White and D.W. Brenner, *Surf. Sci. Lett.*, 316 (1994) L1055.
- [41] U. Starke, A. Barbieri, N. Materer, M.A. Van Hove and G.A. Somorjai, *Surf. Sci.*, 286 (1993) 1, and references cited therein.
- [42] E.A. Carter and B.E. Koel, *Surf. Sci.*, 226 (1990) 339.

- [43] R.S. Taylor and B.J. Garrison, *Chem. Phys. Lett.*, 230 (1994) 495.
- [44] R.S. Taylor and B.J. Garrison, *J. Am. Chem. Soc.*, 116 (1994) 4465.
- [45] (a) R.G. Nuzzo and D.L. Allara, *J. Am. Chem. Soc.*, 105 (1983) 4481.
(b) C.D. Bain and G.M. Whitesides, *Angew. Chem. Int. Ed. Engl.*, 101 (1989) 522.
(c) G.M. Whitesides and P.E. Laibinis, *Langmuir*, 6 (1990) 87.
(d) L.H. Dubois and R.G. Nuzzo, *Annu. Rev. Phys. Chem. Soc.*, 43 (1992) 437.
- [46] C.D. Frisbie, J.R. Martin, R.R. Duff and M.S. Wrighton, *J. Am. Chem. Soc.*, 11 (1992) 7142.
- [47] M.J. Tarlov and J.G. Newman, *Langmuir*, 8 (1992) 1398.
- [48] R.S. Taylor, C.L. Brummel, N. Winograd, B.J. Garrison and J.C. Vickerman, *Chem. Phys. Lett.*, in press.
- [49] M.J.S. Dewar and W. Thiel, *J. Am. Chem. Soc.*, 99 (1977) 4899.
- [50] Y.L. Ha and B.J. Garrison, unpublished results.